Journal of Alloys and Compounds 511 (2012) 35–40

Contents lists available at SciVerse ScienceDirect

Journal of Alloys and Compounds

journal homepage: www.elsevier.com/locate/jallcom

Synthesis, crystal structures, and optical properties of NaCd*Pn*S_3 (*Pn* = As, Sb)

Yuandong Wu, Wolfgang Bensch*

Institut für Anorganische Chemie, Universität Kiel, Max-Eyth-Str. 2, D-24118 Kiel, Germany

ARTICLE INFO

Article history:
Received 30 May 2011
Received in revised form 29 August 2011
Accepted 30 August 2011
Available online 10 September 2011

Keywords:
Alkali polythioarsenate (-antimonate) flux
Cadmium thioarsenate (-antimonate)
Crystal structures
Spectroscopic properties

ABSTRACT

Two compounds NaCd*Pn*S_3 (*Pn* = As (**1**), Sb (**2**)) were synthesized as transparent yellow and red platelets by reacting cadmium powder with the molten mixtures of $Na_2S/As_2S_3/S$ and $Na_2S/Sb/S$ at 500 °C. Both compounds are plagued with crystal twinning and acceptable crystal structure refinement could only be obtained by identifying the type of the twinning laws. $NaCdAsS_3$ (**1**) crystallizes in the monoclinic space group $P2_1/n$ (no. 14) with $a = 5.6561(8)$, $b = 16.5487(15)$, $c = 5.6954(8)$ Å, $\beta = 90.315(11)°$, and $Z = 4$. $NaCdSbS_3$ (**2**) crystallizes in the monoclinic space group $C2/c$ (no. 15) with $a = 8.1329(6)$, $b = 8.1296(4)$, $c = 17.2600(13)$ Å, $\beta = 103.499(6)°$, and $Z = 8$. The structures of both compounds feature a $^2{}_\infty[CdPnS_3]^-$ layer composed of $[CdS_4]$ tetrahedra and $[AsS_3]$ or $[SbS_3]$ pyramidal units. Between the $^2{}_\infty[CdPnS_3]^-$ (*Pn* = As, Sb) layers the Na^+ cations reside in a distorted octahedral environment of S atoms. Compound **1** is characterized with UV/Vis diffuse reflectance spectroscopy and IR and Raman spectra.

1. Introduction

Group 15 chalcogenides are very interesting not only because of their potential application as thermoelectric materials, such as Sb_2Te_3 [1], $AgPb_{18}SbTe_{20}$ [2], $Mo_3Sb_5Te_2$ [3], and $AgSb_xBi_{3-x}S_5$ [4], and nonlinear optical materials, such as $AAsQ_2$ (*A* = Li, Na; *Q* = S, Se) [5,6], $A_3Ta_2AsS_{11}$ (*A* = K, Rb) [7], $AZrPQ_6$ (*A* = K, Rb, Cs; *Q* = S, Se) [8,9], but also because of their structural diversity [10], which arises partly from the various local coordination environments centered by group 15 elements. Unlike its heavier homologues Sb and Bi, trivalent arsenic exhibits a remarkable reluctance to adopt hypervalent coordination polyhedra in its chalcogenido anions [11,12]. The most prominent anions are the pyramidal $[As^{III}Q_3]^{3-}$ and tetrahedral $[As^{V}Q_4]^{3-}$ anions, observed in ternary or quaternary compounds [13–30]. Other anionic moieties include pyramidal $[As^{III}Q_4]^{3-}$ and $[As^{III}Q_5]^{3-}$ [31], which contain *Q*–*Q* dumbbells, and their condensed oligomeric forms such as $[As_2Q_5]^{4-}$ [16], $[As_3Q_6]^{3-}$ [16,24], and $[As_4Q_8]^{4-}$ [20] anions. The structures containing $[As^{III}Q_3]_n^{3-}$ (*n* = 2, 3, 4) units are expected to exhibit a unique structural chemistry due to the stereochemically active As^{III} $4s^2$ lone pair.

To date the most successful synthetic approach for the formation of ternary or quaternary chalcogenoarsenates has been the hydro- (solvento-) thermal technique. However, little work about polychalcogenoarsenate fluxes has been reported. Recently we have reported several quaternary rare earth chalcogenoarsenates, $K_3Ln(AsS_4)_2$ (*Ln* = Nd, Sm Gd, Dy) [32,33], $KEuAsS_4$, $Rb_4Nd_{0.67}(AsS_4)_2$ [33], $K_2Ln_2As_2Se_9$ (*Ln* = Sm, Gd) [34], and $K_3BiAs_6Se_{12}$ [35] prepared in polychalcogenoarsenate fluxes. There is a remarkable difference between the reactivity of arsenic in alkali polysulfide and in polyselenide fluxes. In selenoarsenates predominantly the +3 state of As is favored, whereas the +5 state is more stable in thioarsenates as proved by the frequent occurrence of the $[AsS_4]^{3-}$ anion. This difference is due to the different oxidation power of polysulfide anions compared to polyselenide anions. The considerable structural diversity in the class of chalcogenoarsenate compounds is attributed to various binding modes and reactivities of chalcogenoarsenate anions in the molten flux to coordinate lanthanoide metals or other trivalent metals such as In and Bi [24,36]. Other reaction systems like *A*–*M*–*Pn*–*Q* (*A* = alkali metals; *M* = Zn, Cd, Hg; *Pn* = As, Sb; *Q* = S, Se) are also very interesting because the influence of the charge of the cations and of the stereoactivity of the lone electron pairs can be studied. The initial experiment with group 12 metals in alkali metal thioarsenate flux yielded $Rb_4CdAs_2S_9$ [37], in which the discrete dimeric $[Cd_2(AsS_4)_2(AsS_5)_2]^{8-}$ clusters are composed of two octahedral Cd^{2+} ions bridged by two $[AsS_3(S_2)]^{3-}$ units and chelated each by a $[AsS_4]^{3-}$ unit.

Here, we report the reactivity of Cd in sodium polythio-arsenate and -antimonate fluxes affording salts containing two different two-dimensional $^2{}_\infty[CdAsS_3]^-$ and $^2{}_\infty[CdSbS_3]^-$ anionic layers.

2. Experimental

2.1. Reagents

The reagents employed in this work were used as obtained: Na_2S powder, 98%, Aldrich; Cd powder, −100 mesh, 99.99%, Chempur; S powder, 99.99%, Heraeus; As_2S_3, 99.9%, ABCR; Sb powder, −100 mesh, 99.5%, Aldrich; *N*,*N*-dimethylformamide

* Corresponding author. Tel.: +49 431 880 2091; fax: +49 431 880 1520.
E-mail address: wbensch@ac.uni-kiel.de (W. Bensch).

0925-8388/$ – see front matter © 2011 Elsevier B.V. All rights reserved.
doi:10.1016/j.jallcom.2011.08.102

(DMF), industrial reagent grade, BASF; diethylether, analytical reagent grade, anhydrous, 99.8%, Fluka.

2.2. Synthesis

$NaCdAsS_3$ (**1**) and $NaCdSbS_3$ (**2**) were prepared by reacting a mixture of Na_2S, Cd, As_2S_3 or Sb, and additional S powder in 2:1:1:4 and 1:1:1:8 molar ratio, respectively. The mixtures were thoroughly mixed in a N_2-filled glove box and loaded into a glass ampoule. After evacuation to $\sim 10^{-3}$ mbar the ampoule was flame sealed and placed in a computer-controlled furnace. The mixtures were heated to 500 °C at a rate of 0.5 °C/min, kept at this temperature for 4 days before the sample was cooled down to 100 °C at a rate of 3 °C/h, then the furnace was switched off to cool to room temperature. The products were washed with dry *N*,*N*-dimethylformamide and diethylether yielding transparent yellow platelets (yield about 70% based on Cd for 1) and dark red platelets (yield about 50% based on Cd for 2). The single crystals are stable in DMF, pure ethanol, dry air for up to two months. EDX analyses performed on freshly cleaved faces of several crystals indicated the presence of all four elements (Na, Cd, As (Sb), S) and for all crystals the average compositions are $Na_{1.1}CdAs_{1.0}S_{3.0}$ and $Na_{1.2}CdSb_{1.1}S_{3.2}$. Attempts to replace cadmium with zinc resulted in mixtures of binary and ternary compounds, namely ZnS, Na*Pn*S_2 (*Pn* = As, Sb) [5,38,39].

2.3. Crystal structure determination

The crystal structures of **1** and **2** were determined by single crystal X-ray diffraction methods. Preliminary examination and data collection were performed on a Stoe Imaging Plate Diffraction System (IPDS-2) using graphite-monochromatized Mo Kα radiation (λ = 0.71073 Å) at room temperature. Size of crystal **1**: 0.14 mm × 0.09 mm × 0.04 mm, crystal **2**: 0.15 mm × 0.11 mm × 0.07 mm. The raw data were treated in the usual way applying Lorentz, polarization, and numerical absorption corrections. The initial positions for all atoms were obtained using direct methods, and the structures were refined by full-matrix least-squares techniques with the use of the Shelxtl crystallographic software package [40].

$NaCdAsS_3$ (**1**). The systematic absences pointed to the space group $P2_1/n$. All atoms were found to occupy general positions. A refinement with anisotropic displacement parameters for all atoms led to $R_1 = 0.1644$ and $wR_2 = 0.3237$. A pseudomerohedral twinning was confirmed by using the TwinRotMat program within the Platon package [41], which found two twin components related by the twin law (1, 0, 0; 0, −1, 0; 0, 0, −1) or (−1, 0, 0; 0, −1, 0; 0, 0, 1) with ratio of 0.67/0.33. The final refinement converged with a residual factor of $R_1 = 0.0473$, $wR_2 = 0.1234$ (all data). The maximum and minimum peaks on the final Fourier difference map corresponded to 1.508 and −1.452 $e^-/Å^3$.

$NaCdSbS_3$ (**2**). The space group $C2/c$ was determined on the basis of systematic absences and intensity statistics. One antimony atom, one sodium atom, and three sulfur atoms were found to occupy general positions, while two cadmium atoms were situated on two special positions. A refinement with anisotropic displacement parameters for all atoms led to $R_1 = 0.1230$ and $wR_2 = 0.3296$. To improve the refinement a twin law (0, −1, 0; −1, 0, 0; −½, ½, −1) was used. The final refinement converged with a residual factor of $R_1 = 0.0793$, $wR_2 = 0.1797$ (all data). The maximum and minimum peaks on the final Fourier difference map corresponded to 2.883 and −2.838 $e^-/Å^3$.

An attempt to refine the structure in the non-centrosymmetric space group *C*2 did not improve the results. A symmetry check performed with the ADDSYM option [42] in Platon package [41] always suggests space group $C2/c$.

Technical details of the data acquisition as well as some refinement results are summarized in Table 1. Atomic coordinates and equivalent isotropic displacement parameters and occupancies of atoms are given in Table 2 ($NaCdAsS_3$) and Table 3 ($NaCdSbS_3$). Selected bond lengths and angles are listed in Table 4 ($NaCdAsS_3$) and Table 5 ($NaCdSbS_3$).

Further details of the crystal structure investigation can be ordered referring to the depository No CSD 423525 ($NaCdAsS_3$) and CSD 423526 ($NaCdSbS_3$), the authors and the citation of this paper at the Fachinformationszentrum Karlsruhe, Gesellschaft für wissenschaftlich-technische Information mbH, D-76344 Eggenstein-Leopoldshafen (Germany). E-mail: crysdata@fiz-karlsruhe.de

2.4. Physical measurements

2.4.1. Infrared spectroscopy

Infrared spectrum of compound **1** in the MIR region (4000–400 cm^{-1}, 2 cm^{-1} resolution) was recorded on a Genesis FT-spectrometer (ATI Mattson). The sample was ground with dry KBr into fine powder and pressed into transparent pellet. The infrared spectrum in the far-IR region (550–80 cm^{-1}) was collected on an ISF-66 device (Bruker) with the sample pressed in a polyethylene pellet.

2.4.2. Raman spectroscopy

The Raman spectrum of compound **1** was recorded on an ISF-66 spectrometer (Bruker) equipped with an additional FRA 106 Raman module. A Nd/YAG laser was used as source (λ = 1064 nm). The sample was ground and prepared on an Al sample holder. The measuring range was −1000 to 3500 cm^{-1} (resolution: 2 cm^{-1}).

Table 1
Technical details of data acquisition and some refinement results for $NaCdPnS_3$ (*Pn* = As, Sb).

Empirical formula	$NaCdAsS_3$	$NaCdSbS_3$
Formula weight/g/mol	306.49	353.32
Crystal system	Monoclinic	Monoclinic
Space group	$P2_1/n$ (no.14)	$C2/c$ (no.15)
a/Å	5.6561(8)	8.1329(6)
b/Å	16.5487(15)	8.1296(4)
c/Å	5.6954(8)	17.2600(13)
β/°	90.315(11)	103.499(6)
V/Å^3	533.09(12)	1109.66(13)
Z	4	8
Calc. density/g cm^{-3}	3.819	4.230
Crystal color	Yellow	Red
μ/mm^{-1}	11.339	9.741
F(000)	560	1264
2θ range	$5° \le 2\theta \le 54°$	$5° \le 2\theta \le 54°$
Index range	$-7 \le h \le 7$ $-20 \le k \le 21$ $-7 \le l \le 7$	$-10 \le h \le 10$ $-10 \le k \le 10$ $-22 \le l \le 22$
Goodness-of-fit on F^2	1.032	1.205
Final R for $F_o > 4\sigma(F_o)$[a,b]	$R_1 = 0.0473$, $wR_2 = 0.1180$	$R_1 = 0.0793$, $wR_2 = 0.1789$
R indices for all reflections[a,b]	$R_1 = 0.0548$, $wR_2 = 0.1234$	$R_1 = 0.0811$, $wR_2 = 0.1797$
$\Delta\rho$ ($eÅ^{-3}$)	1.508/−1.452	2.883/−2.838

[a] see $R_1 = \sum ||F_o| - |F_c|| / \sum |F_o|$.

[b] see $wR_2 = \left[\sum w(F_o^2 - F_c^2)^2 / \sum w(F_o^2)^2\right]^{1/2}$, $w = \left[1/\sum(F_o^2) + (aP)2 + bP\right]$, where $P = (\max(F_o^2, 0) + 2Fc^2)/3$.

Table 2
Atomic coordinates and equivalent isotropic displacement parameters U_{eq} ($Å^2 \times 10^3$) for $NaCdAsS_3$. Estimated standards deviations are given in parentheses. The U_{eq} is defined as one third of the trace of the orthogonalized U_{ij} tensor.

	x	y	z	U_{eq}
Cd	0.0013(1)	0.2506(1)	0.2485(1)	31(1)
As	0.4892(1)	0.3990(1)	0.2311(2)	26(1)
S(1)	0.0335(4)	0.1000(1)	0.3391(4)	28(1)
S(2)	0.0914(3)	0.4027(1)	0.2720(5)	27(1)
S(3)	0.0335(4)	0.2371(1)	0.7849(5)	27(1)
Na	0.5333(7)	0.0739(2)	0.2659(8)	38(1)

Table 3
Atomic coordinates and equivalent isotropic displacement parameters U_{eq} ($Å^2 \times 10^3$) for $NaCdSbS_3$. Estimated standards deviations are given in parentheses. The U_{eq} is defined as one third of the trace of the orthogonalized U_{ij} tensor.

	x	y	z	U_{eq}
Sb	0.1760(2)	0.1262(2)	0.5930(1)	20(1)
Cd(1)	0	0.1112(3)	1/4	29(1)
Cd(2)	0	0.6131(3)	1/4	37(1)
S(1)	0.0545(9)	0.0652(7)	0.4025(3)	34(1)
S(2)	0.4071(7)	0.0732(6)	0.0949(3)	25(1)
S(3)	0.2494(7)	0.3329(7)	0.2582(3)	28(1)
Na	0.1597(13)	0.3527(13)	0.0777(3)	37(1)

Table 4
Selected bond distances (Å) and angles (°) for $NaCdAsS_3$. Estimated standard deviations are given in parentheses.

Cd–S(1)	2.551(3)	Cd–S(2)	2.572(2)
Cd–S(3)	2.657(3)	Cd–S(3)	2.663(2)
As–S(1)	2.248(3)	As–S(2)	2.264(2)
As–S(3)	2.286(2)	Na–S(2)	2.860(5)
Na–S(1)	2.890(5)	Na–S(1)	2.892(5)
Na–S(2)	2.925(5)	Na–S(2)	2.927(5)
Na–S(3)	3.130(5)		
S(1)–Cd–S(2)	158.71(8)	S(1)–Cd–S(3)	96.53(7)
S(2)–Cd–S(3)	96.84(8)	S(1)–Cd–S(3)	97.40(8)
S(2)–Cd–S(3)	96.78(7)	S(3)–Cd–S(3)	99.04(8)
S(1)–As–S(2)	102.60(10)	S(1)–As–S(3)	97.35(10)
S(2)–As–S(3)	96.97(9)	As–S(1)–Cd	100.65(9)
As–S(2)–Cd	99.48(8)	As–S(3)–Cd	101.98(10)
As–S(3)–Cd	99.96(9)	Cd–S(3)–Cd	98.30(8)

Table 5
Selected bond distances (Å) and angles (°) for $NaCdSbS_3$. Estimated standard deviations are given in parentheses.

Sb–S(1)	2.451(6)	Sb–S(2)	2.476(5)
Sb–S(3)	2.519(5)	Cd(1)–S(1)	2.593(6) × 2
Cd(1)–S(3)	2.692(6) × 2	Cd(2)–S(2)	2.627(5) × 2
Cd(2)–S(3)	2.739(6) × 2	Na–S(2)	2.794(13)
Na–S(1)	2.852(12)	Na–S(1)	2.963(9)
Na–S(2)	2.982(12)	Na–S(2)	3.003(12)
Na–S(3)	3.034(9)		
S(1)–Sb–S(2)	99.7(2)	S(1)–Sb–S(3)	93.19(19)
S(2)–Sb–S(3)	94.11(18)	S(1)–Cd(1)–S(1)	163.4(3)
S(1)–Cd(1)–S(3)	95.64(19) × 2	S(1)–Cd(1)–S(3)	95.44(17) × 2
S(3)–Cd(1)–S(3)	96.0(3)	S(2)–Cd(2)–S(2)	165.8(2)
S(2)–Cd(2)–S(3)	93.91(16)	S(2)–Cd(2)–S(3)	95.34(17) × 2
S(2)–Cd(2)–S(3)	93.91(16)	S(3)–Cd(2)–S(3)	98.5(3)
Sb–S(1)–Cd(1)	99.9(2)	Sb–S(2)–Cd(2)	97.54(19)
Sb–S(3)–Cd(1)	98.13(19)	Sb–S(3)–Cd(2)	97.70(17)
Cd(1)–S(3)–Cd(2)	96.96(19)		

2.4.3. Solid-state ultraviolet (UV)–visible(Vis)–near-IR spectroscopy

Optical diffuse reflectance measurement was performed at room temperature using a UV–VIS–NIR two-channel spectrometer Cary 5 from Varian Techtron Pty., Darmstadt. The spectrometer is equipped with an Ulbricht sphere (diffuse reflectance accessory; Varian Techtron Pty.). The inner wall of the Ulbricht sphere (diameter 110 mm) is covered with a PTFE layer of 4 mm thickness. A PbS detector (NIR) and a photomultiplier (UV/Vis) are attached to the Ulbricht sphere. The sample was ground with $BaSO_4$ (as standard for 100% reflectance) and prepared as a flat specimen. The resolution was 1 nm for the UV/Vis range and 2 nm for the near-IR range. The measuring range was 250–2000 nm. Absorption (α/S) data were calculated from the reflectance spectra using the Kubelka–Munk function [43]: $\alpha/S = (1-R)^2/2R$, where R is the reflectance at a given wave-number, α is the absorption coefficient, and S is the scattering coefficient. The band gap was determined as the intersection point between the energy axis at the absorption offset and the line extrapolated from the linear part of the absorption edge in a $(\alpha/S)^2$ vs. E (eV) plot.

3. Results and discussion

3.1. Synthesis

Compound **1** was prepared by using a flux ratio of 2:1:1:4 for $Na_2S/Cd/As_2S_3/S$ at 500 °C. The influence of flux basicity on the reaction product was also explored. A change in the flux basicity was achieved by altering the Na_2S/S ratio. The compound is not formed in less basic flux, for example, the products from the flux with a molar ratio of 1:1:4 for $Na_2S/As_2S_3/S$ (formally "$Na_2As_2S_8$") are $NaAsS_2$ [5] and CdS. The products obtained under more basic conditions were also investigated. Applying a flux with a molar ratio of 3:1:4 for $Na_2S/As_2S_3/S$ ("$Na_6As_2S_{10}$") compound **1** was not formed and CdS and a glassy red amorphous product were observed.

In the antimony system, an alteration of the flux ratio also changed the reaction product but it did not parallel the products in the arsenic system except for $NaCdSbS_3$ (**2**), which is the arsenic analogue and was formed from a flux with 1:1:1:8 of $Na_2S/Cd/Sb/S$. Increasing the ratio of $Na_2S/Sb/S$ from 1:1:8 to 4:1:8, phase 2 was no longer formed. Instead the compounds Na_3SbS_4 and CdS were obtained.

3.2. Crystal structures

The structure of $NaCdAsS_3$ (**1**) consists of two-dimensional $^2{}_\infty[CdAsS_3]^-$ layers and Na^+ cations. These layers are perpendicular to [0 1 0] and are repeated every $b/2$ in the [0 1 0] direction. The Na^+ ions are located between the anionic layers bonded to six S neighbors (Fig. 1). Each anionic layer is made up of tetrahedral $[CdS_4]^{6-}$ units and $[AsS_3]^{3-}$ trigonal pyramids (Fig. 2). The Cd^{2+} cation is surrounded by four S^{2-} anions in a distorted tetrahedral arrangement. Each $[CdS_4]^{6-}$ tetrahedron shares two corners with two adjacent tetrahedra to form a one-dimensional $[CdS_3]$ chain directed

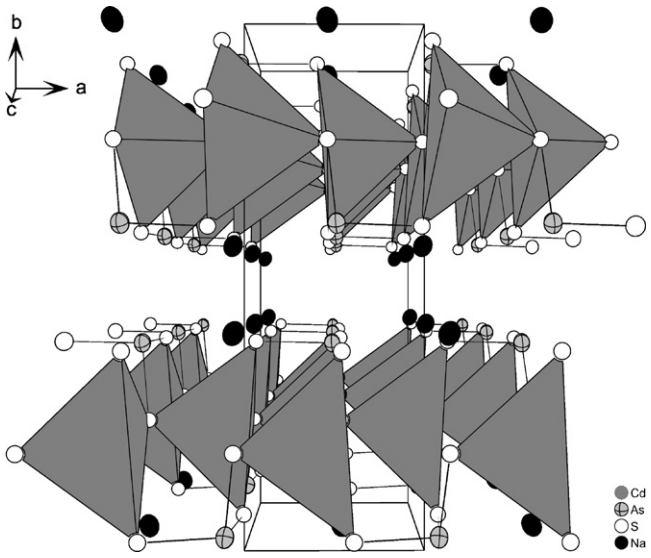

Fig. 1. Crystal structure of $NaCdAsS_3$ viewed along [0 0 1]. The $[CdS_4]$ tetrahedra are displayed as polyhedra for clarity. The displacement ellipsoids are drawn at the 50% probability level.

along [1 0 $\bar{1}$]. Parallel chains are joined by $[AsS_3]^{3-}$ moieties in an up–down manner to form the two-dimensional $^2{}_\infty[CdAsS_3]^-$ layer. As a result of the connection scheme, each $[CdS_4]^{6-}$ tetrahedron is connected to four $[AsS_3]^{3-}$ trigonal pyramids. The Cd–S bond lengths are normal, ranging from 2.551(3) to 2.663(2) Å with an average of 2.611 Å. The S–Cd–S angles ranging from 96.53(7) to 158.71(8)° indicate a severe distortion of the tetrahedral coordination geometry. In $Na_6Cd_7S_{10}$ [44] the four crystallographically unique Cd^{2+} cations possess tetrahedral coordination with different degrees of distortions. For two Cd^{2+} ions the Cd–S bond lengths vary between 2.528 and 2.632 Å (S–Cd–S angles: 101.7–114.3°) while

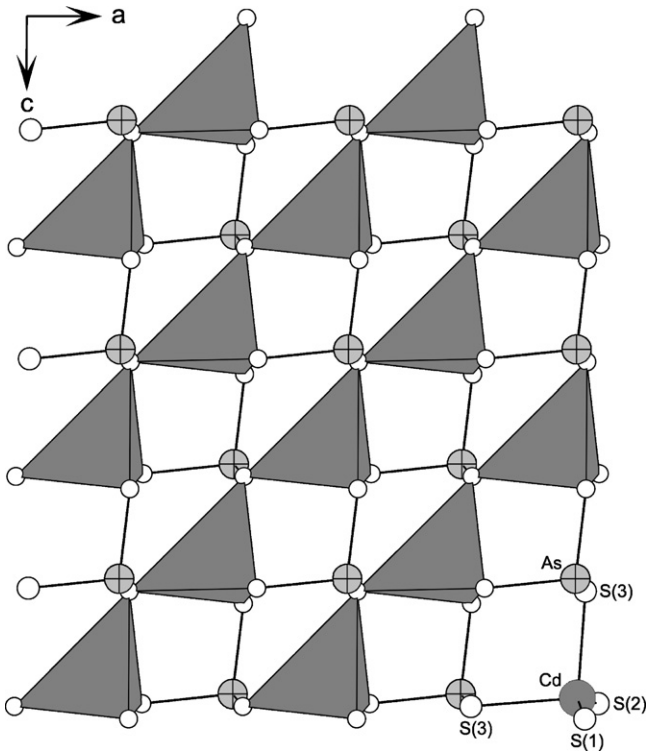

Fig. 2. View of one $^2{}_\infty[CdAsS_3]^-$ layer with an atomic labeling scheme down the [0 1 0] direction.

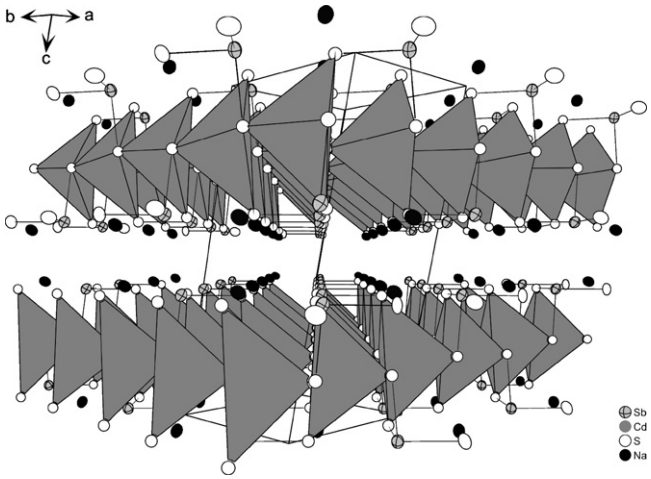

Fig. 3. Crystal structure of $NaCdSbS_3$ viewed along [1 1 0]. The [CdS_4] tetrahedra are displayed as polyhedra for clarity. The displacement ellipsoids are drawn at the 50% probability level.

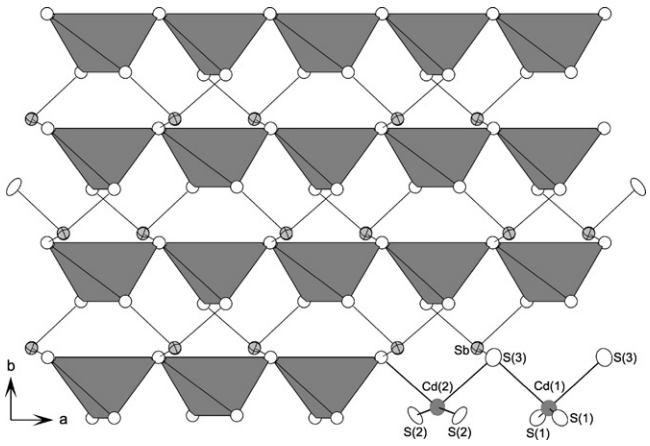

Fig. 4. View of one $^2{}_\infty[CdSbS_3]^-$ layer with an atomic labeling scheme down the [0 0 1] direction.

for the other two Cd^{2+} cations the Cd–S bonds range from 2.526 to 2.783 Å and corresponding S–Cd–S angles between 90.8 and 120.9°. Whereas the Cd–S bond lengths are similar to those in compound **1**, the S–Cd–S angles scatter in a narrower range than in **1**.

The $[AsS_3]^{3-}$ trigonal pyramid is similar to that found in many other thioarsenates like e.g. $AEuAsS_3$ (A = Li, K, Rb, Cs) [45]. The As–S bond lengths of 2.248(3), 2.264(2), and 2.286(2) Å belong to the "non-bridge" category described by Takeuchi et al. [46]. The S–As–S bond angles of 96.97(9), 97.35(10), and 102.60(10)° (mean: 98.97°) correspond very well to those in $KSnAsS_5$ [31]. The next nearest S neighbors are located at a distance longer than 3.35 Å which is too far apart for As–S bonding interactions. Each S(1) and S(2) atom has only two nearest neighbors: one Cd atom and one As atom, whereas the S(3) atom has three nearest neighbors: two Cd^{2+} and one As^{3+} cation. This difference in coordination of sulfur atoms is reflected in the Cd–S(3) bond lengths of 2.657(3) and 2.663(2) Å compared to Cd–S(1) and Cd–S(2) bonds of 2.551(3) and 2.572(2) Å, respectively.

The arrangement of the S^{2-} anions around the Na^+ cation shows a distorted octahedral coordination geometry, with six Na–S contacts ranging from 2.860(5) to 3.130(5) Å with an average of 2.938 Å, which is slightly longer than the sum of effective ionic radii of Na^+ and S^{2-}, 2.86 Å [47]. This coordination mode for sodium is often observed in alkali thioarsenates such as in Na_3AsS_3 [48] with Na–S distances from 2.830 to 3.132 Å, or $NaAsS_2$ [5] exhibiting Na–S bond lengths between 2.815 and 3.061 Å. The Na^+ cations are loosely packed in the space between two anionic layers. A similar arrangement is found in the structure of synthetic christite $TlHgAsS_3$ [49], where the Tl^+ ions are located between the layers consisting of $[AsS_3]^{3-}$ trigonal pyramids and mercury atoms. However, the shortest Tl–Tl distance is 3.39 Å while the shortest Na–Na distance in **1** amounts to 3.64 Å. The former distance is similar to the Tl–Tl separation in elemental thallium (3.40 Å) [50], and the Tl atoms may provide the principal cohesive force between the layers.

The crystal structure of $NaCdSbS_3$ (**2**) contains the same structural motif as compound **1**, i.e., $^2{}_\infty[CdSbS_3]^-$ anionic layers. However, the unit cell of compound **2** contains two crystallographically unique Cd^{2+} ions. The structure consists of trigonal pyramids $[SbS_3]^{3-}$ linked by cadmium atoms to form a two-dimensional layer network. They are parallel to (0 0 1) and occur every $c/2$ in the [0 0 1] direction as shown in the Fig. 3. Again, the Na^+ cations are located between the layers in a distorted octahedral environment.

The Sb atom is coordinated by three sulfur atoms to form a slightly distorted trigonal pyramid (Fig. 4). The Sb–S bond lengths are 2.451(6) Å for Sb–S(1), 2.476(5) Å for Sb–S(2) and 2.519(5) Å for Sb–S(3). These bond lengths are typical for $[SbS_3]^{3-}$ pyramids found in compounds such as Tl_3SbS_3 (Sb–S: 2.430 Å) [51], KSb_5S_8 (Sb–S: 2.423–2.515 Å), parapierrotite, $TlSb_5S_8$ (Sb–S: 2.440–2.488 Å) [52] or in a large number of other thioantimonates(III) [53–55]. The bond lengths in **2** agree well with the sum of covalent radii of Sb and S (2.439 Å) [47]. In contrast to the Sb–S bonding situation in $KHgSbS_3$ [56], the Sb–S(3) bond in **2** is slightly longer than the other two Sb–S bonds, even though S(1) and S(2) form strong covalent bonds to two Cd^{2+} cations at 2.593(6) and 2.627(5) Å, respectively, while S(3) seems to have weaker bonding interactions to Cd^{2+} (2.692(6) × 2 and 2.739(6) × 2 Å) (Fig. 4). The S–Sb–S bond angles of 99.7(2)°, 93.19(19)°, and 94.11(18)° (mean: 95.67°) are slightly larger than the mean value of 94.6° for sulfosalts calculated by Takeuchi et al. [46], and are much smaller than those (mean: 98.4°) found in $KHgSbS_3$ [56]. The Sb atom has three further S neighbors at longer distances (3.249–3.322 Å) leading to a distorted octahedral geometry characterized by a 3 + 3 coordination. The extension of the coordination number of Sb in thioantimonates(III) is well documented and often leads to coordination which may be described as 3 + n with n = 1–3 [57–60]. In **2** two of the Sb–S contacts are within the layer and one is to an S atom of a neighbored layer. Considering the latter Sb–S distance as a weak bonding interaction the layers are interconnected into a three-dimensional network.

The two unique Cd^{2+} ions, Cd(1) and Cd(2), are located on the two-fold axis in the structure, and are coordinated by four S^{2-} anions in distorted tetrahedral geometry. The Cd–S bond lengths can be divided into two groups. The short Cd–S bonds at 2.593(6) Å (×2) and 2.692(6) Å (×2) yield a nearly linear geometry: S(1)–Cd(1)–S(1) = 163.4(3)°, S(2)–Cd(2)–S(2) = 165.8(2)°, and two long Cd(1)–S(3) and Cd(2)–S(3) bonds are at 2.692(6) and 2.739(6) Å, respectively. The former two bond lengths compare well with the sum for covalent radii of tetrahedrally coordinated Cd^{2+} and S^{2-} of 2.62 Å [47], while the latter two are longer than this value. In sulfides the Cd^{2+} cations mainly adopt a tetrahedral environment. But to the best of our knowledge there are some exceptions: in $Cd_2Sb_6S_{11}$ [61], $CdPS_3$ [62] and $CdInS_2$ [63] Cd^{2+} cations are octahedrally coordinated and in $BaCdS_2$ [64] Cd^{2+} is triangular planar coordinated. A careful inspection shows that in $CdPS_3$ [62] and $CdInS_2$ [63], the [CdS_6] octahedra are distorted with Cd–S bond lengths from 2.709 to 2.740 Å in $CdPS_3$ (S–Cd–S angles between 85.56 and 175.60°) and Cd–S bonds of 2.669 Å and corresponding S–Cd–S angles between 84.90 and 180° in $CdInS_2$. In the compound $Cd_2Sb_6S_{11}$ [61] a more severe distortion of the octahedron is observed with S atoms at 2.592, 2.610 × 2, 2.662, and 2.825 × 2 Å. The latter two distances are significantly longer than the sum of covalent radii of Cd and S (2.62 Å [47]). In compounds **1** and **2**, the

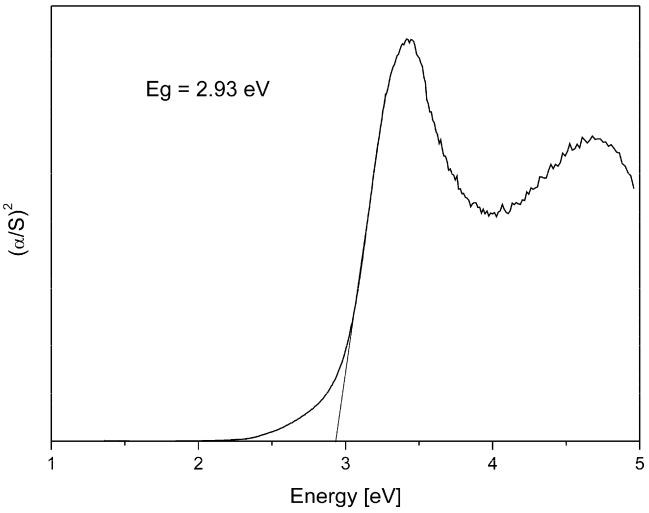

Fig. 5. Transformed reflectance UV/vis spectrum of $NaCdAS_3$.

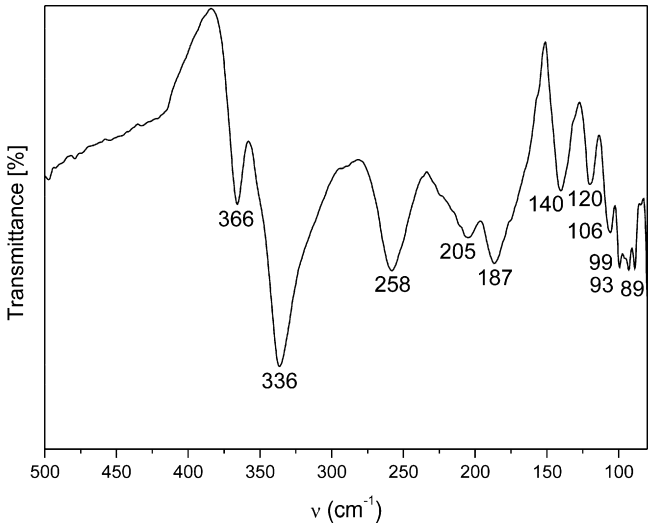

Fig. 6. Far-IR spectrum of $NaCdAsS_3$.

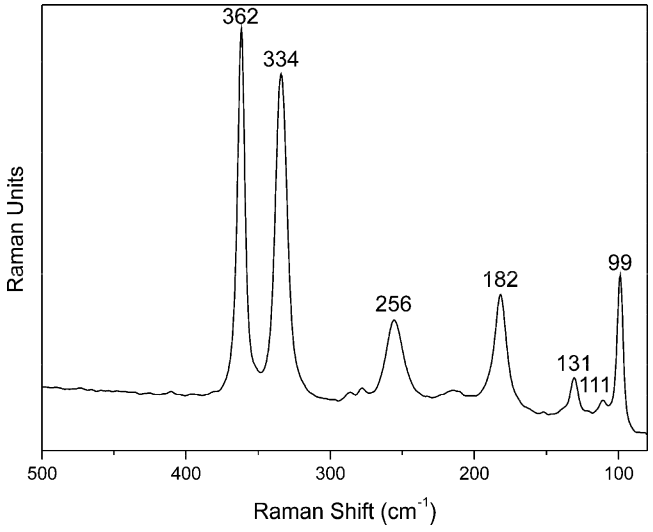

Fig. 7. FT-Raman spectrum of $NaCdAsS_3$.

closest distance between the Cd^{2+} ions in one unit and S^{2-} anions in the neighboring units are 3.070(6) Å, and 3.031(6) Å, respectively. If these weak Cd–S interactions are considered, the coordination polyhedra appear to be distorted octahedra or pseudo-octahedra.

The Na^+ ion is surrounded by six S^{2-} anions forming a distorted octahedron with Na–S distances ranging from 2.794 (13) to 3.034(9) Å. The average Na–S bond in **2** of 2.936 Å agrees with the value found for compound **1**.

3.3. Optical properties

The solid state diffuse reflectance UV/vis spectrum of compound **1** (Fig. 5) displays a very steep and strong absorption edge corresponding to a band gap of ~2.93 eV consistent with the transparent yellow color. This is attributed to excitations within the $^2{}_\infty[CdAsS_3^-]$ layer and supposed to originate from transitions involving an electronic charge-transfer excitation from the top of the valence band (VB) to the bottom of the conduction band (CB), where the uppermost part of the valence band can be presumably attributed to filled S-based *p* orbitals and the bottom of the conduction band results most likely from empty Cd-based *s* orbitals. The Na^+ cation does not seem to play a significant role in defining the electronic structure of the framework, consistent with the predominantly ionic character of the Na. . .*S* interactions. Compared to the band-gap of $AEuAsS_3$ (A = K, Rb, Cs) [45] (E_g = 2.0 eV) with a layered anion, the value is increased by ~0.9 eV in compound **1**.

The far-IR and Raman spectra for $NaCdAsS_3$ in the range from 80 to 500 cm^{-1} are displayed in Figs. 6 and 7. The FIR spectrum exhibits absorptions at 366, 336, 258, 205, 187, 140, 120, 106, 99, 93, and 89 cm^{-1}, and the Raman spectrum shows resonances at 362, 334, 256, 182, 131, 111, and 99 cm^{-1}. In accordance with the mode predictions made by factor group analysis [$6A_1 + 7A_2 + 13E$], six modes of A_1 symmetry and 13 modes of *E* symmetry are observed in the IR and Raman spectra of proustite [65]. Due to the similar structural properties, the similar types and number of spectral modes are expected in the IR and Raman spectra of compound **1**. It is well known that for this type of compounds with complex structures, the selection of a unique polyatomic vibrational group to whose the observed IR and Raman bands could be attributed is not a straightforward task. In spite of that, in our previous work [32,33], the interpretation of the IR and Raman spectra was based on the presence of $[MS_n]$ polyhedra (here $[AsS_3]^{3-}$ trigonal pyramids) as main vibrational units. Compared to IR and Raman spectra of proustite, the strong absorption modes at 366, 336, and 258 cm^{-1} in the IR spectrum and very strong peaks at 362, 334, and 256 cm^{-1} in the Raman spectrum are attributed to the symmetric stretching of pyramidal $[AsS_3]^{3-}$ groups. The bands at 205, 187 cm^{-1} (IR) and 182 cm^{-1} (Raman) are probably mainly due to deformation modes which could be mixed with the $\nu(Cd^{II}–S)$ modes. These values are shifted to slightly lower frequencies compared to those in $KEuAsS_3$ [45] because of the weaker As–S interactions following from the longer As–S bonds. The remaining three weak bands at 131, 111, and 99 cm^{-1} in the Raman spectrum and six weak absorptions in the IR (140, 120, 106, 99, 93, 89 cm^{-1}) may be assigned to the Cd–S stretching and the S–Cd–S bending vibrations or result from collective lattice modes.

4. Conclusions

The quaternary compounds $NaCdAsS_3$ and $NaCdSbS_3$ were synthesized by the reactive flux method. The layered anion $^2{}_\infty[CdPnS_3]^-$ contains severely distorted $[CdS_4]^{6-}$ tetrahedra and pyramidal $[PnS_3]^{3-}$ anions. The two compounds are not isostructural which is normal comparing the structures of thioarsenates and thioantimonates. This observation may be explained by the very different stereochemical activity of the lone electron pairs of As^{3+} and Sb^{3+} as well as by the tendency of Sb^{3+} to enhance the

coordination number beyond three. In the structure of $NaCdSbS_3$ the Sb atom is in a 3 + 3 coordination and a weak interlayer Sb–S contact generates a three-dimensional network. The compound $NaCdSbS_3$ was synthesized in a sulfur-rich sodium polyantimonate flux with relative low Lewis basicity, while $NaCdAsS_3$ was formed at a higher Lewis basicity. These conditions seem to be essential for the stabilization of the compounds because increasing or decreasing the flux basicity result in formation of simpler compounds. Although the synthesis of compounds containing specific ligands $[Pn_xS_y]^{n-}$ would be hard to control interesting compounds can be expected applying fluxes with different compositions and properties.

Acknowledgement

Financial support by the DFG (Deutsche Forschungsgemeinschaft) is gratefully acknowledged.

Appendix A. Supplementary data

Supplementary data associated with this article can be found, in the online version, at doi:10.1016/j.jallcom.2011.08.102.

References

[1] T. Thonhauser, T.J. Scheidemantel, J.O. Sofo, J.V. Badding, G.D. Mahan, Phys. Rev. B 68 (2003) 085201.
[2] K.F. Hsu, S. Loo, F. Guo, W. Chen, J.S. Dyck, C. Uher, T. Hogan, E.K. Polychroniadis, M.G. Kanatzidis, Science 303 (2004) 818.
[3] E. Dashjav, A. Szczepenowska, H. Kleinke, J. Mater. Chem. 12 (2002) 345.
[4] J.H. Kim, D.Y. Chung, D. Bilc, S. Loo, J. Short, S.D. Mahanti, T. Hogan, M.G. Kanatzidis, Chem. Mater. 17 (2005) 3606.
[5] T.K. Bera, J.H. Song, A.J. Freeman, J.I. Jang, J.B. Ketterson, M.G. Kanatzidis, Angew. Chem. Int. Ed. 47 (2008) 7828.
[6] T.K. Bera, J.I. Jang, J.H. Song, C.D. Malliakas, A.J. Freeman, J.B. Ketterson, M.G. Kanatzidis, J. Am. Chem. Soc. 132 (2010) 3484.
[7] T.K. Bera, J.I. Jang, J.B. Ketterson, M.G. Kanatzidis, J. Am. Chem. Soc. 131 (2009) 75.
[8] S. Banerjee, J.M. Szarko, B.D. Yuhas, C.D. Malliakas, L.X. Chen, M.G. Kanatzidis, J. Am. Chem. Soc. 132 (2010) 5348.
[9] S. Banerjee, C.D. Malliakas, J.I. Jang, J.B. Ketterson, M.G. Kanatzidis, J. Am. Chem. Soc. 130 (2008) 12270.
[10] Y.D. Wu, W. Bensch, CrystEngComm 12 (2010) 1003.
[11] W.S. Sheldrick, M. Wachhold, Coord. Chem. Rev. 176 (1998) 211.
[12] A. Kromm, T. van Almsick, W.S. Sheldrick, Z. Naturforsch. B 65 (2010) 918.
[13] V. Vater, W.S. Sheldrick, Z. Naturforsch. B 53 (1998) 1259.
[14] M. Wachhold, W.S. Sheldrick, Z. Naturforsch. B 51 (1996) 32.
[15] M. Wachhold, W.S. Sheldrick, Z. Naturforsch. B 52 (1997) 169.
[16] M. Wachhold, M.G. Kanatzidis, Inorg. Chem. 38 (1999) 3863.
[17] M. Wachhold, M.G. Kanatzidis, Inorg. Chem. 38 (1999) 4178.
[18] M. Wachhold, M.G. Kanatzidis, Inorg. Chem. 39 (2000) 2337.
[19] J.A. Hanko, J.H. Chou, M.G. Kanatzidis, Inorg. Chem. 37 (1998) 1670.
[20] J.H. Chou, J.A. Hanko, M.G. Kanatzidis, Inorg. Chem. 36 (1997) 4.
[21] M.G. Kanatzidis, J.H. Chou, J. Solid State Chem. 127 (1996) 186.
[22] J.H. Chou, M.G. Kanatzidis, J. Solid State Chem. 123 (1996) 115.
[23] J.H. Chou, M.G. Kanatzidis, Inorg. Chem. 33 (1994) 5372.
[24] J.H. Chou, M.G. Kanatzidis, Inorg. Chem. 33 (1994) 1001.
[25] G.L. Schimek, J.W. Kolis, Acta Crystallogr. C 53 (1997) 991.
[26] J.E. Jerome, P.T. Wood, W.T. Pennington, J.W. Kolis, Inorg. Chem. 33 (1994) 1733.
[27] S.C. Oneal, W.T. Pennington, J.W. Kolis, Inorg. Chem. 31 (1992) 888.
[28] S.C. Oneal, W.T. Pennington, J.W. Kolis, J. Am. Chem. Soc. 113 (1991) 710.
[29] F. Pertlik, Monatsh. Chem. 125 (1994) 1311.
[30] F. Pertlik, J. Solid State Chem. 112 (1994) 170.
[31] R.G. Iyer, M.G. Kanatzidis, Inorg. Chem. 41 (2002) 3605.
[32] Y.D. Wu, C. Näther, W. Bensch, Inorg. Chem. 45 (2006) 8835.
[33] Y.D. Wu, W. Bensch, Solid State Sci. 11 (2009) 1542.
[34] Y.D. Wu, W. Bensch, Inorg. Chem. 48 (2009) 2729.
[35] Y. Wu, W. Bensch, J. Alloys Compd. 509 (2011) 4452.
[36] M. Wachhold, M.G. Kanatzidis, Z. Anorg, Allg. Chem. 626 (2000) 1901.
[37] R.G. Iyer, M.G. Kanatzidis, Inorg. Chem. 43 (2004) 3656.
[38] K. Volk, H. Schäfer, Z. Naturforsch. B 33 (1978) 827.
[39] A.S. Kanishcheva, V.G. Kuznetsov, V.N. Batog, J. Struct. Chem. 20 (1979) 122.
[40] G.M. Sheldrick, Acta Crystallogr. A 64 (2008) 112.
[41] A.L. Spek, J. Appl. Crystallogr. 36 (2003) 7.
[42] Y. Le Page, J. Appl. Crystallogr. 21 (1988) 983.
[43] P. Kubelka, F. Munk, Z. Tech. Phys. 12 (1931) 593.
[44] E.A. Axtell, M.G. Kanatzidis, Chem. Mater. 8 (1996) 1350.
[45] T.K. Bera, M.G. Kanatzidis, Inorg. Chem. 47 (2008) 7068.
[46] Y. Takeuchi, R. Sadanaga, Z. Kristallogr. 130 (1969) 346.
[47] R.D. Shannon, Acta Crystallogr. A 32 (1976) 751.
[48] M. Palazzi, Acta Crystallogr. B 32 (1976) 3175.
[49] K.L. Brown, F.W. Dickson, Z. Kristallogr. 144 (1976) 367.
[50] J.G. Speight, Lang's Handbook of Chemistry, McGraw-Hill, Laramie, Wyoming, 2005.
[51] N. Rey, J.C. Jumas, J. Olivier-Fourcade, E. Philippot, Acta Crystallogr. C 40 (1984) 1655.
[52] P. Berlepsch, R. Miletich, T. Armbruster, Z. Kristallogr. 214 (1999) 57.
[53] V. Spetzler, H. Rijnberk, C. Näther, W. Bensch, Z. Anorg. Allg. Chem. 630 (2004) 142.
[54] V. Spetzler, C. Näther, W. Bensch, Inorg. Chem. 44 (2005) 5805.
[55] B. Seidlhofer, N. Pienack, W. Bensch, Z. Naturforsch. B 65 (2010) 937.
[56] M. Imafuku, I. Nakai, K. Nagashima, Mater. Res. Bull. 21 (1986) 493.
[57] L. Engelke, C. Näther, W. Bensch, Eur. J. Inorg. Chem. (2002) 2936.
[58] L. Engelke, R. Stähler, M. Schur, C. Näther, W. Bensch, R. Pöttgen, M.H. Möller, Z. Naturforsch. B 59 (2004) 869.
[59] M. Schäfer, C. Näther, W. Bensch, Monatsh. Chem. 135 (2004) 461.
[60] W. Bensch, M. Schur, Eur. J. Solid State Inorg. Chem. 34 (1997) 457.
[61] I.P. Deineko, I.K. Egorovtismenko, V.D. Spitsyna, M.A. Simonov, N.V. Belov, Dokl. Akad. Nauk SSSR 254 (1980) 877.
[62] G. Ouvrard, R. Brec, J. Rouxel, Mater. Res. Bull. 20 (1985) 1181.
[63] G.D. Guseinov, G.B. Abdullay, E.M. Kerimova, R.S. Gamidov, G.G. Guseinov, Mater. Res. Bull. 4 (1969) 807.
[64] J.E. Iglesias, K.E. Pachali, H. Steinfink, J. Solid State Chem. 9 (1974) 6.
[65] P. Makreski, G. Jovanovski, L. Minceva-Sukarova, B. Soptrajanov, A. Green, B. Engelen, I. Grzetic, Vib. Spectrosc. 35 (2004) 59.